Lee, M.-H., & Bell, R. M. (1991) *Biochemistry 30*, 1041–1049.
Maekawa, S., & Sakai, H. (1990) *J. Biol. Chem. 265*, 10940–10942.
McLaughlin, S., Mulrine, N., Gresalfi, T., Vaio, G., & McLaughlin, A. (1981) *J. Gen. Physiol. 77*, 445–473.
Mosior, M., & McLaughlin, S. (1991) *Biophys. J. 60*, 149–159.
Newton, A. C., & Koshland, D. E., Jr. (1987) *J. Biol. Chem. 262*, 10185–10188.
Newton, A. C., & Koshland, D. E., Jr. (1989) *J. Biol. Chem. 264*, 14909–14915.
Newton, A. C., & Koshland, D. E., Jr. (1990) *Biochemistry 29*, 6656–6661.
Nishizuka, Y. (1986) *Science 233*, 305–312.
Orr, J. W., & Newton, A. C. (1990) *Biophys. J. 57*, 284a.
Orr, J. W., & Newton, A. C. (1992) *Biochemistry* (preceding paper in this issue).
Palatini, P., Dabbeni-Sala, F., Pitotti, A., Bruni, A., & Mandersloot, J. C. (1977) *Biochim. Biophys. Acta 466*, 1–9.
Parks, W. A., Couper, C. L., & Low, R. L. (1990) *J. Biol. Chem. 265*, 3436–3439.
Perin, M. S., Fried, V. A., Mignery, G. A., Jahn, R., & Südhof, T. C. (1990) *Nature 345*, 260–263.
Politino, M., & King, M. M. (1990) *J. Biol. Chem. 265*, 7619–7622.
Robson, R. J., & Dennis, E. A. (1977) *J. Phys. Chem. 81*, 1075–1078.
Sandermann, H., Jr. (1983) *Trends Biochem. Sci. 8*, 408–411.
Sandermann, H., Jr., McIntyre, J. O., & Fleischer, S. (1986) *J. Biol. Chem. 261*, 6201–6208.
Snoek, G. T., Feijen, A., Hage, W. J., Van Rotterdam, W., & De Laat, S. W. (1988) *Biochem. J. 255*, 629–637.
Tamura, M., Tamura, T., Tyagi, S. R., & Lambeth, J. D. (1988) *J. Biol. Chem. 263*, 17621–17626.
Uratani, Y., Wakayama, N., & Hoshino, T. (1987) *J. Biol. Chem. 262*, 16914–16919.
Yeagle, P. L., Young, J., & Rice, D. (1988) *Biochemistry 27*, 6449–6452.

Comparison of Hydrogen Exchange Rates for Bovine Pancreatic Trypsin Inhibitor in Crystals and in Solution†

Warren Gallagher,‡ Feng Tao, and Clare Woodward*
Department of Biochemistry, University of Minnesota, St. Paul, Minnesota 55108
Received August 22, 1991; Revised Manuscript Received January 30, 1992

ABSTRACT: Hydrogen exchange rate constants for the 17 slowest exchanging amide NH groups in bovine pancreatic trypsin inhibitor (BPTI) were measured in solution and in form II and form III crystals. All 17 amide hydrogens are buried and intramolecularly hydrogen bonded in the crystal structure, except Lys 41 which is buried and hydrogen bonded to a buried water. Large-scale crystallization procedures were developed for these experiments, and rate constants for both crystal and solution exchange were measured by ^{1}H NMR spectroscopy of exchange-quenched samples in solution. Two conditions of pH and temperature, pH 9.8 and 35 °C, and pH 9.4 and 25 °C, bring two groups of hydrogens into the experimental time window (minutes to weeks). One consists of the 10 slowest exchanging hydrogens, all of which are associated with the central β-sheet of BPTI. The second group consists of seven more rapidly exchanging hydrogens, which are distributed throughout the molecule, primarily in a loop or turn. In both groups, most hydrogens exchange more slowly in crystals, but there is considerable variation in the degree to which the exchange is depressed in crystals. Many differences observed for the more rapidly exchanging hydrogens can be attributed to local surface effects arising from intermolecular contacts in the crystal lattice. Within the slower group, however, a very large effect on exchange of Ile 18 and Tyr 35 appears to be selectively transmitted through the matrix of the molecule. Backbone atoms of Ile 18 and Tyr 35 are mutually hydrogen bonded to each other at the open end of a pair of twisted antiparallel β-sheet strands, which are closed at the other end in a hairpin-like arrangement by a short turn. Ile 18 and Tyr 35 exchange rates are slowed by 4–5 orders of magnitude in crystals. Their location in the protein suggests that crystallization selectively damps motions of the open end of the β-sheet, which connects the flexible loops with the more rigid central core of the molecule.

Nitrogen-bound hydrogens in the peptide and side chain amide groups of proteins are labile and exchange with solvent hydrogens. Their exchange kinetics can be measured by the rate of disappearance of amide resonances in ^{1}H NMR[1] spectra, as ^{1}H isotope is replaced by ^{2}H. Isotope exchange rate constants for amide groups in native globular proteins typically vary over many orders of magnitude. Surface amide hydrogens exchange most rapidly, while buried ones exchange with rates that are 3–10 orders of magnitude slower. The fact that buried amide hydrogens in folded proteins eventually exchange implies there are structural fluctuations which provide transient access of interior regions of a protein to water

† This work is supported by NIH Grant GM26242.
‡ Present address: Department of Chemistry, University of Wisconsin-Eau Claire, Eau Claire, WI 54702

[1] Abbreviations: BPTI, bovine pancreatic trypsin inhibitor; NMR, nuclear magnetic resonance; FID, free induction decay.

0006-2960/92/0431-4673$03.00/0

and catalytic hydronium and hydroxyl ions (Linderstrøm-Lang, 1958). In this sense, amide hydrogen exchange kinetics are taken as a measure of internal motions in native proteins. Hydrogen exchange rate constants of buried amide groups are proportional to the submolecular motility in the vicinity of the exchanging group. The molecular details of the fluctuations involved are not certain, and the relative merits of various possibilities have been reviewed (Woodward et al., 1982; Barksdale & Rosenberg, 1982; Englander et al., 1980; Englander & Kallenbach, 1984; Tüchsen & Woodward, 1987a,b).

Here we report a comparison of the hydrogen isotope exchange kinetics of 17 of the slowest exchanging hydrogens in crystal forms of bovine pancreatic trypsin inhibitor (BPTI). Proteins in the crystal state are not static but undergo internal fluctuations, as shown by the temperature dependence of the crystallographic *B* factors (Petsko & Ringe, 1984). Since hydrogen exchange rates of the same amide hydrogen can be measured in solution and in crystals, they provide directly comparable experimental monitors of internal motions in the two states at numerous locations within a protein.

Neutron diffraction studies demonstrate ^1H–^2H exchange in protein crystals. To reduce the background from incoherent neutron scattering by hydrogen atoms, crystals are typically soaked in ^2H_2O for weeks to years prior to collection of the data. Hydrogen and deuterium atoms can be distinguished and located in the structure, and the amide hydrogens protected from isotope exchange for the period of soaking can be identified. Neutron diffraction structures have been reported for several globular proteins, including ribonuclease A (Wlodawer & Sjolin, 1982), trypsin (Kossiakoff, 1982), lysozyme (Mason et al., 1984; Bentley et al., 1983), metmyoglobin (Ragavan & Schoenborn, 1984), crambin (Teeter & Kossiakoff, 1984), and BPTI (Wlodawer et al., 1984). In general, most of the protected amide hydrogens participate in main chain to main chain hydrogen bonds in buried α-helix and β-sheet structures. In BPTI, 11 amide hydrogens are protected from exchange after soaking for 4 months at pH 8.2.

Recently, Pedersen et al. (1991) compared the hydrogen exchange rates of lysozyme in solution and in two crystal forms by NMR. They rank 126 peptide amide groups into one of four categories representing broad ranges of exchange rates (individual exchange rate constants were not determined). For buried amides there is a general slowing of exchange in the lysozyme crystals, but not all are slowed to the same extent. The extent of the reduction in exchange rates in lysozyme crystals is not correlated with proximity to intermolecular contacts. However, it is clear that the lattice contacts alter the internal fluctuations of the protein which allow water and ions to come in contact with amides buried in the interior of the protein (Pedersen et al., 1991). In earlier studies by Tüchsen and Ottesen (1979), comparisons of bulk hydrogen isotope exchange rates were made for lysozyme in crystals and in solution using the radioactive tritium isotope of hydrogen. Similar exchange kinetics were observed for the first 200 min after initiating exchange. Tüchsen and Ottesen (1979) were able to observe exchange for the fastest 60% of the exchangeable hydrogens; the slowest 45 hydrogens did not exchange by 200 min in either solution or crystals.

BPTI has 53 exchangeable peptide amide hydrogens and 4 slowly exchanging asparagine side chain amide protons. Hydrogen isotope exchange rates in solution for most have been published (Wagner & Wüthrich, 1979, 1982; Roder et al., 1985; Woodward & Hilton, 1980; Tüchsen & Woodward, 1985a, 1987a,b). The experiments reported here were designed to ask two questions: Is there a difference in the internal fluctuations of BPTI in solution and crystals as monitored by the slowest one-third of its exchangeable protons? If so, do the effects of crystallization differ significantly between one internal region of the protein and another? Our results give an affirmative answer to both these questions: Exchange rates are generally slower in crystals than in solution, and there is considerable variation in the effect of crystallization on different amide groups. The most striking effect is observed for exchange of the amide hydrogens of Ile 18 and Tyr 35. These residues are at the end of the central β-sheet; the NH of each is hydrogen bonded to the backbone oxygen of the other. The decrease by 4–5 orders of magnitude in Ile 18 and Tyr 35 exchange rates suggests a selective damping of fluctuations at the end of the β-sheet that joins the flexible loops to the rigid, hydrophobic core of the molecule. This is consistent with the results of trypsin binding effects on hydrogen exchange (Brandt & Woodward, 1987) and with the structure of a new variant of BPTI with the Tyr 35 side chain removed (Housset et al., 1991).

Materials and Methods

To compare crystal and solution hydrogen exchange rates for a number of BPTI amides, it was necessary to develop procedures for obtaining large quantities of BPTI crystals. Form II and III crystals of BPTI were grown from 1.5 M K_2HPO_4 using the procedure reported by Wlodawer et al. (1987b). Crystal growth at pH values below 9.4 favors formation of form II crystals, while pH values above 9.4 favor form III crystals.

To initiate the exchange reaction, BPTI crystals in 1.5 M K_2HPO_4 were collected on a Millipore filter (8-μm pore size) and suspended in ^2H_2O containing 1.5 M K_2HPO_4. This marked the starting time for the exchange reaction. The suspensions were kept in a water bath maintained at the desired temperature. The pH of the crystal suspension (uncorrected glass electrode reading) was adjusted to the desired pH at the beginning of the experiment with either ^2HCl or KO^2H. Throughout the experiment the pH was checked and adjusted when necessary. Both form II and III crystals are unstable at pH values below 8.7; this limited our experiments to pH values between 9 and 10. At different times after initiation of exchange, samples of crystals were collected on a Millipore filter and dissolved in ^2H_2O titrated with ^2HCl to pH 3.6 to quench isotope exchange. These solutions were stored at 4 °C until used to obtain the ^1H NMR spectrum. The exchange reactions were carried out for as long as 28 days. This procedure accomplishes two things: first, further exchange from the slowest group of protons is effectively quenched because the exchange process is pH dependent and near its minimum at pH 3.6. And second, the crystals dissolve because both pH and salt concentration are lowered; this permits use of solution NMR techniques to measure exchange rates.

Exchange rates were computed from the decay rate of assigned NH resonances in the ^1H NMR spectrum in ^2H_2O solvent, as described in Tüchsen and Woodward (1985a). Spectra were collected on General Electric 300- and 500-MHz spectrometers. Solvent resonances were suppressed by selective irradiation prior to the data acquisition pulse. The FID's were collected in either 8K or 16K blocks. To smooth the spectra and increase the apparent resolution, the FID's were multiplied by a double exponential before transforming to the frequency domain. The temperature was maintained at either 25 or 40 °C during data collection.

To make the resonance assignments, we ran a crystal experiment on form III crystals at pH 9.0 and 22 °C and collected two time points: one at 0.10 h and one at 1.88 h. These

Table I: Hydrogen Isotope Exchange Rates for Amide Protons in BPTI in Solution and Form III Crystals

	pH 9.8, 35 °C			pH 9.4, 25 °C		
residue	k_{soln} (h^{-1})	k_{xtal} (h^{-1})	k_{soln}/k_{xtal}	k_{soln} (h^{-1})	k_{xtal} (h^{-1})	k_{soln}/k_{xtal}
Glu 7				2.9×10 (± 3)[b]	7×10^{-1} ($\pm 2 \times 10^{-1}$)	4×10 (± 10)
Ile 18	2.1×10 (± 2)[a]	2.9×10^{-3} ($\pm 2 \times 10^{-4}$)	7.5×10^{3} ($\pm 1 \times 10^{3}$)	3.3 ($\pm 3 \times 10^{-1}$)[b]	$<3 \times 10^{-4}$	$>1 \times 10^{4}$
Arg 20	8×10^{-2} ($\pm 1 \times 10^{-2}$)	5.2×10^{-4} ($\pm 8 \times 10^{-5}$)	1.5×10^{2} ($\pm 4 \times 10$)			
Tyr 21	$<1 \times 10^{-3}$	$<2 \times 10^{-4}$				
Phe 22	$<1 \times 10^{-3}$	$<2 \times 10^{-4}$				
Tyr 23	2.4×10^{-3} ($\pm 5 \times 10^{-4}$)	3.6×10^{-3} ($\pm 4 \times 10^{-4}$)	6.7×10^{-1} ($\pm 2 \times 10^{-1}$)			
Asn 24	1.3 ($\pm 2 \times 10^{-1}$)	3.6×10^{-1} ($\pm 5 \times 10^{-2}$)	4 (± 1)		2.6×10^{-2} ($\pm 7 \times 10^{-3}$)	
Gly 28				3.4×10^{3} ($\pm 3 \times 10^{2}$)[b]	1.0 ($\pm 5 \times 10^{-1}$)	3×10^{3} ($\pm 2 \times 10^{3}$)
Leu 29				7.2 ($\pm 7 \times 10^{-1}$)[b]	1.7×10^{-1} ($\pm 4 \times 10^{-2}$)	4×10 ($\pm 2 \times 10$)
Gln 31	8.1×10^{-1} ($\pm 5 \pm 10^{-2}$)	4.6×10^{-1} ($\pm 7 \times 10^{-2}$)	1.8 ($\pm 4 \times 10^{-1}$)	9.6×10^{-2} (1×10^{-2})[c]	6.1×10^{-2} ($\pm 2 \times 10^{-3}$)	1.6 ($\pm 2 \times 10^{-1}$)
Phe 33	1.0×10^{-1} ($\pm 1 \times 10^{-2}$)	6.0×10^{-4} ($\pm 2 \times 10^{-4}$)	1.7×10^{2} ($\pm 7 \times 10$)			
Tyr 35	3.2×10 (± 3)[a]	2.1×10^{-4} ($\pm 9 \times 10^{-5}$)	1.5×10^{5} ($\pm 1 \times 10^{4}$)	5.0 ($\pm 5 \times 10^{-1}$)[b]	$<3 \times 10^{-4}$	$>2 \times 10^{4}$
Gly 36				2.6×10 (± 3)[b]	1.9×10^{-1} ($\pm 5 \times 10^{-2}$)	1.4×10^{2} ($\pm 5 \times 10$)
Lys 41				7.8×10^{2} ($\pm 8 \times 10$)[b]	4.8×10^{-2} ($\pm 9 \times 10^{-3}$)	1.6×10^{4} ($\pm 5 \times 10^{3}$)
Phe 45	1.0×10^{-1} ($\pm 1 \times 10^{-2}$)	$<2 \times 10^{-4}$	$>5 \times 10^{2}$			
Asn 44				2.8 ($\pm 3 \times 10^{-1}$)[b]	1.1×10^{-1} ($\pm 4 \times 10^{-2}$)	3×10 (± 10)
Asn 43 N_δHe	6.0×10^{-1} ($\pm 1 \times 10^{-1}$)	6.6×10^{-3} ($\pm 3 \times 10^{-4}$)	9×10 ($\pm 2 \times 10$)			
Asn 43 N_δHz	6.8×10^{-1} ($\pm 4 \times 10^{-2}$)	6.8×10^{-3} ($\pm 5 \times 10^{-4}$)	1.0×10^{2} (± 10)			
Cys 51				5.0×10 (± 5)[b]	2	2.5×10 (± 3)

[a] Calculated from rates obtained at lower pH values in 0.3 M KCl at 25 °C assuming first-order [OH^-] dependence, no salt concentration dependence, and an activation enthalpy of $\Delta H^* = 17$ kcal/mol. [b] Calculated from rates obtained at lower pH values in 0.3 KCl at 25 °C assuming first-order [OH^-] dependence and no salt concentration dependence. [c] Calculated from rate obtained at pH 9.8, 35 °C assuming first-order [OH^-] dependence and an activation enthalpy of $\Delta H^* = 17$ kcal/mol.

samples were used to obtain 2-D COSY spectra. The spectra were collected using the procedure described by Wagner and Wüthrich (1982), and assignments were taken from that paper.

To make the comparison of solution and crystal rate constants as unambiguous as possible, solution exchange measurements of the slowest exchanging protons were carried out under the same conditions of pH and salt concentration as the crystal exchange experiments. Lyophilized BPTI was dissolved in ^2H_2O, titrated to pH 3, and placed on ice. The solution was warmed to the experimental temperature, and an equal volume of 3.0 M K_2HPO_4 was added to give a final concentration of 1.5 M K_2HPO_4. The added 3.0 M K_2HPO_4 was made with ^2H_2O and preequilibrated at the experimental temperature and pH. The addition of the 3.0 M phosphate buffer marked the zero time for the exchange reaction. Because the solubility of BPTI in 1.5 M K_2HPO_4 is less than 1 mg/mL, it is not possible to obtain NMR spectra directly with the exchanging solution. To get around this, a sample of the exchanging solution was removed at various times after the initiation of exchange and the protein in the sample collected by precipitation. This was accomplished by increasing the concentration of K_2HPO_4 to 2.0 M with the addition of solid K_2HPO_4. The precipitated protein was collected on a Millipore filter (8-μm pore size) and dissolved in ^2H_2O with ^2HCl added to give a final pH of 3.6. The final protein concentration was approximately 10 mg/mL. These solutions were stored at 4 °C until the spectra were obtained. Prior to ^1H NMR spectroscopy, the protein solutions were filtered with a Millipore Millex GV filter (0.22-μm pore size) to removed any undissolved protein. Exchange rate constants were obtained from the decay of ^1H NMR resonances as described above.

Results

Table I shows the observed exchange rate constants for amide hydrogens of BTPI in form III crystals and in solution at pH 9.8 and 35 °C, and at pH 9.4 and 25 °C. These two conditions bring different protons into the observational time window and allow us to distinguish two groups of exchanging protons, the slowest exchanging group in the crystal (rate constants in the range 10^{-4}–10^{-1} h^{-1} at pH 9.8, 35 °C) and the next slowest exchanging group in the crystal (rate constants in the range 10^{-2}–2 h^{-1} at pH 9.4, 25 °C). Under the conditions of these experiments, hydrogen isotope exchange is catalyzed by hydroxyl ions and governed by a low activation energy mechanism (Woodward et al., 1982; Tüchsen & Woodward, 1987b).

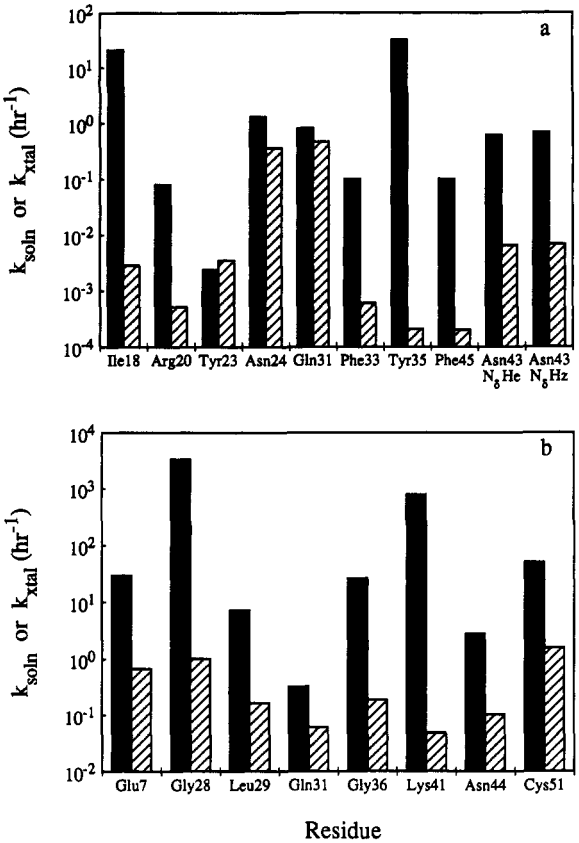

FIGURE 1: Solution (solid bars) and crystal (cross-hatched bars) hydrogen isotope exchange rates for individual amide hydrogens in BPTI at (a) pH 9.8 and 35 °C and (b) pH 9.4 and 25 °C. All are peptide amide hydrogens except for Asn 43 $N_\delta H_e$ and Asn 43 $N_\delta H_z$, which are primary amide hydrogens of the Asn 43 side chain.

The slowest exchanging group comprises peptide amides in the central region of the β-sheet along with the side chain amide of Asn 43. These include the peptide amides of residues 18, 20, 23, 24, 31, 33, 35, and 45 and the H_e ($H^{\gamma 21}$) and Hz ($H^{\gamma 22}$) hydrogens of Asn 43 side chain. A graphical comparison of the solution and crystal rates for this group is shown in Figure 1a. In addition, the slowest exchanging group also includes two other amide protons of the central β-sheet, Tyr 21 and Phe 22, which exchange too slowly to measure in either solution or crystals at pH 9.8, 35 °C. The second group consists of the next fastest exchanging peptide amides in the crystal, those of residues 7, 28, 29, 36, 41, 44, and 51 (Gln 31 exchange can be measured under both conditions), and comparison of the solution and crystal rates for these is shown in Figure 1b. In general, the crystallization slows the rate of exchange; however, there is a high degree of variation in the extent of slowing. For example, the amide hydrogens of Ile 18 and Try 35 (Figure 1a) have exchange rates 4–5 orders of magnitude slower in the crystal than in solution, while the peptide amide protons of other β-sheet residues 23, 24, and 31, show little difference. No amide hydrogens were observed to exchange significantly slower in solution than in crystals. Although the actual exchange rate constant measured for Tyr 23 is slightly larger in the crystal (Table I), we do not consider the difference to be significant.

The hydrogen exchange rates for the slowest group of amide hydrogens of BPTI in solution were obtained under the same conditions of pH, temperature, and salt concentration as the mother liquor in the crystals. For the more rapidly exchanging amide hydrogens (Figure 1b), the solution rates are too fast to measure by the methods described for the slowest exchanging protons. For this group in Figure 1b, the solution

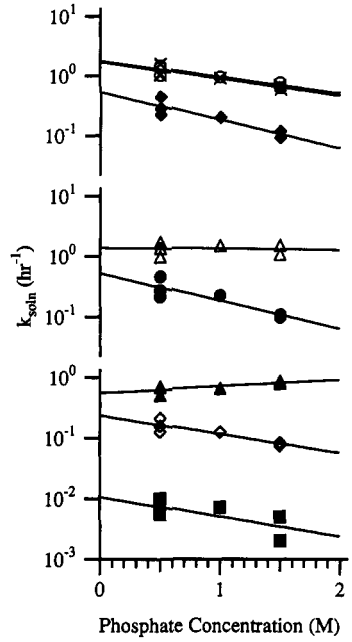

FIGURE 2: Phosphate concentration dependence of the hydrogen isotope exchange rates for individual amide hydrogens of BPTI in solution at pH 9.8 and 35 °C: ■, Tyr 23; ◇, Arg 20; ▲, Gln 31; ●, Phe 45; △, Asn 24; ◆, Phe 33; ×, Asn 43 $N_\delta H_e$; and ○, Asn 43 $N_\delta H_z$.

rates (Table I) were extrapolated from a complete data set obtained at 25 °C over the pH range of 2–8.5 in 0.3 M KCl by assuming first-order catalysis by hydroxyl ions (J. van Pelt and C. Woodward, unpublished results). There are additional amide hydrogens that exchange with solution rates similar to those shown in Figure 1b, but they were not observed in the crystal experiments. Figure 1b, therefore, indicates the members of this group that are selectively slowed in the crystal.

Amide hydrogen exchange rates are highly sensitive to pH and temperature and may vary with salt concentration (Tüchsen & Woodward, 1985b). Since the salt dependence of hydrogen exchange is not well characterized, we determined the phosphate concentration dependence of the solution rates at pH 9.8 for the slowest exchanging group of protons. The results are shown in Figure 2. There appears to be little or no salt dependence for many of the amides; while for others there appears to be a slight decrease in the exchange rate at the higher salt concentrations in solution. On the basis of these observations, we think it is appropriate to use the solution data collected at lower salt concentrations for the comparison with the crystal data collected at pH 9.4 and 25 °C.

Four crystal forms have been reported for BPTI (Crick, 1953; Huber et al., 1970; Walter & Huber, 1983; Wlodawer et al., 1987b). Our most complete data set, summarized in Table I, was obtained with form III crystals, whose crystallization in 1.5 M K_2HPO_4 is favored at pH values above 9.4. Form III crystals were stable for the duration of the experiments (about 1 month): examination of the crystals throughout the experiments by light microscopy showed no detectable change in morphology. Form II crystals were also studied (data not shown). It is significant that none of the faster group observed in form III crystals (those in Figure 1b) were observed in form II crystals when the first time point was taken (after 15 min of exchange at pH 9, 35 °C). That is, these NH hydrogens, including Gly 28 and Lys 41, exchange far more rapidly in form II than in form III crystals. In contrast, effects of crystallization on the slow group (those in Figure 1a) are very similar for form II and form III crystals, including the marked slowing of Ile 18 and Tyr 35. However,

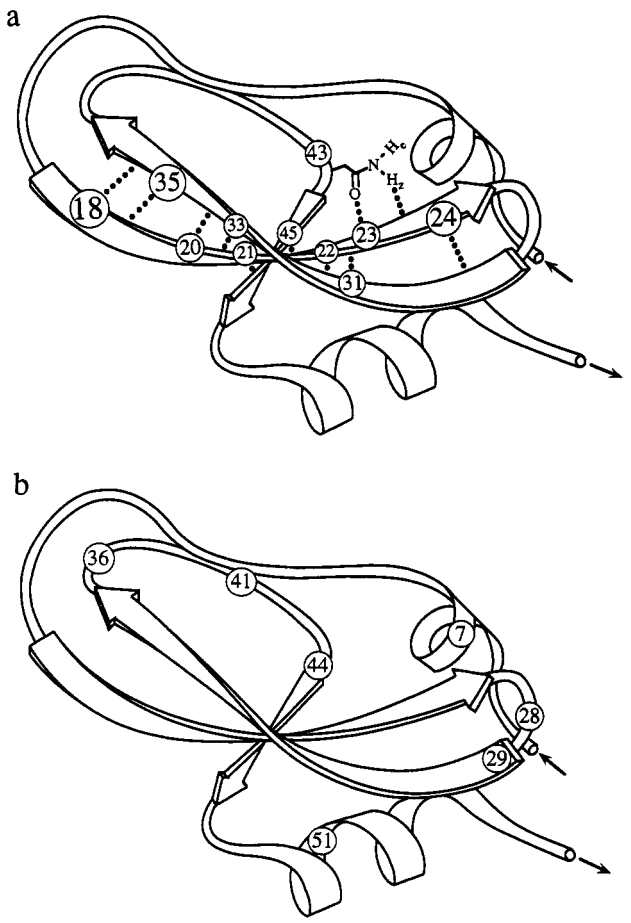

FIGURE 3: Richardson drawings of BPTI showing the location of the amides included in this study. The residues are labeled at the position of the peptide nitrogen, and dots show the direction of the hydrogen bonds. (a) The slowest group of exchanging amide hydrogens measured at pH 9.8 and 35 °C. (b) The faster exchanging group of amide hydrogens in the crystal measured at pH 9.4 and 35 °C. [Figures were adapted from Figure 53 in Richardson (1981) and used with permission of the author.]

since form II crystals begin to crack after a couple of weeks at 35 °C, we did not pursue a detailed characterization of exchange in form II.

Discussion

All of the amide hydrogens monitored in this study are buried and intramolecularly hydrogen bonded, with the exception of Lys 41 NH which is buried and hydrogen bonded to a buried water. All have zero solvent accessibility in the crystal structure (Lee & Richards, 1971), and their exchange is many orders of magnitude slower than equivalent amide hydrogens which are fully exposed to solvent. However, since they do have measurable hydrogen exchange rates, these amide groups have a *dynamic* accessibility to solvent in both crystals and solution; on average they are buried and hydrogen bonded, but occasional conformational fluctuations expose them to solvent components and lead to isotope exchange.

The most conspicuous feature of BPTI tertiary structure is a twisted central β-sheet consisting of two contiguous, antiparallel strands (residues 18–24 and 29–35), plus a third short strand (residues 45–46), as indicated in the Richardson drawing (Figure 3). In a hairpin-like arrangement, the two longer antiparallel strands are connected by a short turn. Two helices, one at the N-terminus and one at the C-terminus, are packed against the closed end of the hairpin. Finally, the molecule contains two long, overlapping, aperiodic loops, residues 7–17 and 36–44, which enclose four buried water molecules (not shown). These water molecules accept and donate hydrogen bonds to buried protein NH and O atoms which are too distant to hydrogen bond directly to each other [see Wlodawer et al. (1987a) and Tüchsen et al. (1987)]. Figure 3a shows the locations of the slowest exchanging protons, those observed at pH 9.8 and 35 °C (exchange rates in Figure 1a). Figure 3b shows the locations of the those exchanging next in the crystal, the group observed at pH 9.4 and 25 °C (exchange rates in Figure 1b).

The crystal lattice interactions in form III BPTI crystals involve nine protein-to-protein intermolecular hydrogen bonds with symmetry related molecules (Table 3 in Wlodawer et al., 1987b). For seven of these, the donors are on lysine or arginine side chains. One is the N-terminal arginine residue, five are found in the loops (residues 15, 17, 39, 41, and 42), and the remaining one is in the C-terminal helix (residue 53). The other two donors are the backbone amide nitrogens of Lys 15 and Arg 39. Six of the acceptors are peptide carbonyl oxygen atoms (residues 8, 25, 27, 28, 39, and 44), and three are side chain oxygen atoms (residues 7, 11, and 49). No intermolecular hydrogen bonds are located in the vicinity of Tyr 35 and Ile 18 backbone amide hydrogens. Figure 4 shows the packing of BPTI molecules in the unit cell of form III crystals; the side chains at the major contact sites, those of residues 15, 17, 39, 41, and 42, are displayed in bold on the right.

Comparison of the solution versus crystal exchange rates shown in Figure 1 may be summarized in two points. (1) All of the protons are slower exchanging in crystals than in solution, except Tyr 23, which is about the same in both. (2) Four amide hydrogens are slower by more than 3 orders of magnitude: Ile 18, Tyr 35, Gly 28, and Lys 41. Since the differences between solution and crystal exchange rates are due to crystal lattice contacts, the question of interest is whether the effects of these contacts are propagated through the molecule by changes in internal fluctuations or due to local, surface perturbations at the intermolecular contacts. The general slowing of exchange in crystals supports the idea that many motions responsible for hydrogen exchange in BPTI are damped in the crystal. In addition, there are the very large localized effects on residues 18, 35, 28, and 41 to explain.

Considering first Gly 28 and Lys 41, their slowed exchange in form III crystals is most likely due to surface effects at lattice contact points. Both are in the faster exchanging group, shown in Figure 1b. Members of this group are not clustered in one locale but spread throughout the molecule (Figure 3b), in the turn (28 and 29), one of the loops (36, 41, and 44), and on the interior sides of the two helices (7 and 51). Both Gly 28 and Lys 41 are at a major contact region in form III crystals, as shown in Figure 4. Lys 41 peptide amide is located in the center of the loop which runs from residue 36 to 44 and which is involved in the major crystal lattice contact across the 2-fold crystallographic axis with the same loop on a symmetry related molecule. Four of the protein-to-protein intermolecular hydrogen bonds are included in this interaction, and they involve the backbone carbonyl oxygens of Arg 39 and Asn 44, the backbone amide nitrogen of Arg 39, and side chain nitrogens of Arg 39, Lys 41, Arg 42, and Asn 44. Figure 4 (right) is centered on the side chains of 39, 41, and 42 at this extensive lattice contact region surrounding Lys 41 NH. Also shown are the side chains of Lys 15 and Arg 17, which pack against the region of Gly 28 in neighboring molecules. Gly 28 peptide amide is surrounded by three protein-to-protein intermolecular hydrogen bonds, all of which involve backbone carbonyl oxygens (Ala 25, Ala 27, and Gly 28) hydrogen

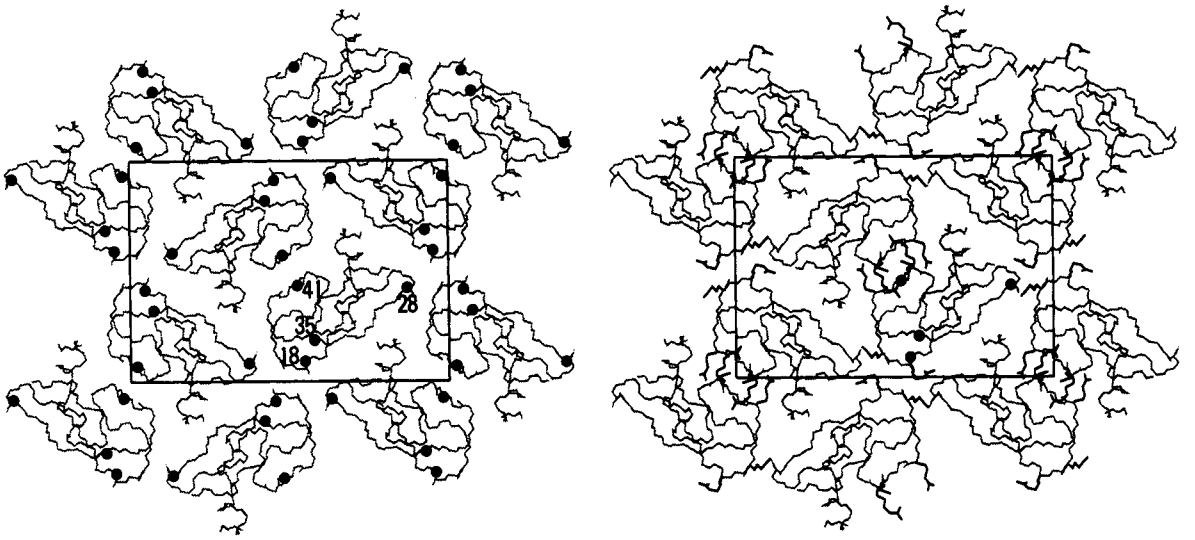

FIGURE 4: Packing of BPTI molecules in crystal form III. (Left figure) Backbone C, CA, and N atoms are shown in projection down the crystallographic *c* axis. Closed circles indicate the NH of Ile 18, Tyr 35, Gly 28, and Lys 41. (Right figure) Side chains at the two major contact sites are shown in bold. The reciprocal contacts of the side chains of Arg 39, Lys 41, and Arg 42 are in the center and at the corners of the box. The side chains of Lys 15 and Arg 17 are along the edges of the box. Closed circles mark the location of 18, 35, 28, and 41 NH in one molecule. BPTI form III structure is reported in Wlodawer et al. (1987b).

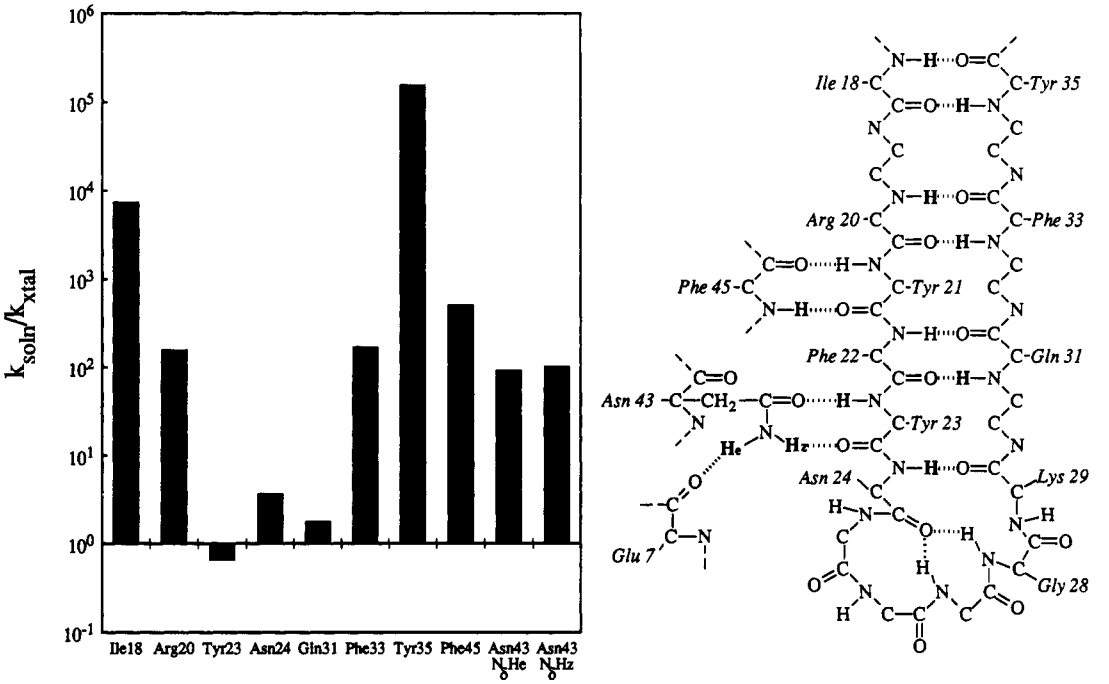

FIGURE 5: Ratio of the solution hydrogen isotope exchange rate to the crystal hydrogen isotope exchange rate for the slowest group of amide hydrogens in BPTI, along with the chemical structure of the β-sheet region of BPTI showing the location of these amide hydrogens.

bonded to the side chains of Lys 15 and Arg 17. Besides Gly 28 and Lys 41, the other protons in Figure 1b include Leu 29, Gly 36, and Asn 44, also located near the two lattice contacts just described, and Glu 7, whose side chain participates in a protein-to-protein intermolecular hydrogen bond.

The conclusion that the slowing of Lys 41 and Gly 28 is due to surface effects at the lattice contact points is supported by our studies carried out on form II crystals at pH 9.0 and 35 °C, where exchange rates should be equivalent to those at pH 9.4 and 25 °C. All of the amide hydrogens in the second group for form III were completely exchanged by the first time point (15 min) in form II crystals. If Gly 28 and Lys 41 exchanged as slowly in form II as in form III crystals, they should be observed during the first couple of hours of exchange. In form II crystals there are fewer and less extensive lattice contacts and only four protein-to-protein intermolecular hydrogen bonds: Ala 24 O–Arg 17 NH, Ala 27 O–Tyr 35 side chain OH, and Asn 44 O and Arg 42 O both hydrogen bonded the guanidino group of Arg 39 (Wlodawer et al., 1987a).

In contrast to Lys 41 and Gly 28, the very slow exchange of Ile 18 and Tyr 35 is observed in both crystal forms. In solution, the Ile 18 and Tyr 35 amides are among the most rapidly exchanging protons in the β-sheet, while in the form II and III crystals they are among the slowest in the molecule (Figure 1a). Their exchange in the crystal is slowed by a factor of 10^4 and 10^5, respectively. Surface effects do not explain this suppression of exchange. Intermolecular contacts in either crystal form selectively damps internal motions in the region of Tyr 35 and Ile 18 backbone. The nature of these motions is suggested by other features of BPTI structure and hydrogen exchange rates. These are (1) the overall hydrogen exchange behavior of the protein, (2) the structural changes in a mutant

BPTI in which Tyr 35 is replaced by glycine, (3) the pattern of exchange of the β-sheet hydrogens in crystals, and (4) the selective slowing of hydrogen exchange for the amide hydrogens of Ile 18 and Tyr 35 in the trypsin/BTPI complex and in crystals.

Using the criterion of hydrogen exchange rate as the indicator of flexibility, BPTI contains two clearly distinguishable domains, one of exceptional rigidity and stability and a second of very high flexibility. The rigid region, forming the hydrophobic core of the protein, is identified by the slowest exchanging protons, the peptide amide hydrogens of residues 21, 22, and 23 (Hilton et al., 1981). In contrast, the flexible region composed of the two overlapping loops (7–17, 36–44) is highly mobile compared to the rest of the molecule (Tüchsen et al., 1987a,b). The overlapping loops enclose four buried water molecules which are observable at 100% occupancy in crystals (Wlodawer et al., 1987a). These waters are mobile in solution (Tüchsen et al., 1987; Otting & Wüthrich, 1989) and have residence times of 10^{-2}–10^{-8} s in solution (Otting et al., 1991).

The structure and mobility of the loop region is quite independent of the core region. This is illustrated by the change in the crystal structure of the loops that occurs when Tyr 35, a buried residue in the loop region, is replaced by glycine to form the variant Y35G of BPTI. In naturally occurring BPTI, the backbone amide hydrogens of Tyr 35 and Ile 18 make reciprocal hydrogen bonds: the amide hydrogen of one is hydrogen bonded to the backbone carbonyl oxygen of the other and vice versa (Figure 3a). The 18–35 hydrogen bond pair is at the open end of the hairpin β-sheet structure, where the flexible loops are connected to the rigid core of the molecule. In the high-resolution crystal structure of Y35G, the loops are reordered, with several atoms displaced by >6 Å, but the hydrophobic core of the molecule shows little or no change (Housset et al., 1991). Significantly, in Y35G residues 18 and 35 are not hydrogen bonded to one another in the β-sheet, but instead, the amide nitrogens and carbonyl oxygens of each are hydrogen bonded to a buried water molecule.

The pattern of exchange for the β-sheet protons in crystals indicates that one end of the β-sheet is affected much more than the other. The bar graph in Figure 5 gives the ratio of the solution to crystal rates for the hydrogens in the hairpin β-sheet structure. The U-shape of the bar heights illustrates that the open end of the hairpin is much more affected in the crystal state than the closed end. The amides in the 18–35 hydrogen bond pair at the open end of the hairpin are slowed most; the next hydrogen bond pair, Arg 20 and Phe 33, are affected somewhat less, and further down the β-sheet there is little difference in crystal and solution exchange rates.

Selective slowing of Tyr 35 and Ile 18 amide hydrogens is also the largest effect on hydrogen exchange rates observed when BPTI forms a complex with trypsin, its physiological ligand (Brandt & Woodward, 1987). Trypsin binds to the inhibitor at the overlapping loop region, with Lys 15 of BPTI in the trypsin specificity site.

In conclusion, the selective quenching of amide exchange for Tyr 35 and Ile 18 in crystals and in the trypsin/BPTI complex, taken together with the overall hydrogen exchange characteristics of BPTI and the structure of Y35G BPTI, suggests that the open end of the β-sheet, consisting of the 18–35 hydrogen bond pair, serves as a flexible connection between two submolecular domains. Suppression of hydrogen exchange for the amide hydrogens of residues 18 and 35 by crystallization and by trypsin binding appears to reflect the damping of motions associated with movement of the more mobile active site loops relative to the more rigid hydrophobic core of the protein.

Registry No. BPTI, 9087-70-1; Gln, 56-85-9; Ile, 73-32-5; Arg, 74-79-3; Tyr, 60-18-4; Phe, 63-91-2; Asn, 70-47-3; Gly, 56-40-6; Leu, 61-90-5; Lys, 56-87-1; Cys, 52-90-4.

References

Barksdale, A., & Rosenberg, A. (1982) *Methods Biochem. Anal. 28*, 1–113.

Brandt, P., & Woodward, C. (1987) *Biochemistry 26*, 3156–3162.

Bentley, G., Delepierre, M., Dobson, C., Mason, S., Poulsen, F., & Wedin, R. (1983) *J. Mol. Biol. 170*, 243–247.

Crick, F. H. C. (1953) *Acta Crystallogr. 6*, 221–222.

Englander, S. W., & Kallenbach, N. (1984) *Q. Rev. Biophys. 16*, 521–655.

Englander, S. W., Calhoun, D., Englander, J., Kallenbach, N., Leim, N., Malin, R., Mandal, C. & Rogero, J. (1980) *Biophys. J. 32*, 577–589.

Hilton, B., Trudeau, K., & Woodward, C. (1981) *Biochemistry 20*, 4697–4703.

Housset, D., Kim, K. S., Fuchs, J., Woodward, C., & Wlodawer, A. (1991) *J. Mol. Biol. 220*, 757–770.

Huber, R., Kukla, D., Ruehlmann, A., Epp, O., & Formanek, H. (1970) *Naturwissenschaften 57*, 389–392.

Kossiakoff, A. (1982) *Nature 296*, 713–721.

Lee, B. K., & Richards, F. M. (1971) *J. Mol. Biol. 55*, 379–400.

Linderstrøm-Lang, K. U. (1958) in *Symposium on Protein Structure* (Neuberger, A., Ed.) Methuen, London.

Mason, S., Bentley, G., & McIntyre, G. (1984) *Basic Life Sci. 27*, 323–334.

Otting, G., & Wüthrich, K. (1989) *J. Am. Chem. Soc. 111*, 1871–1875.

Otting, G., Liepinsh, E., & Wüthrich, K. (1991) *J. Am. Chem. Soc. 113*, 4363–4364.

Pedersen, T. G., Sigurskjold, B. W., Andersen, K. V., Kjaer, M., Poulsen, F. M., Dobson, C. M., & Redfield, C. (1991) *J. Mol. Biol. 218*, 413–426.

Petsko, A., & Ringe, D. (1984) *Annu. Rev. Biophy. Bioeng. 13*, 331–372.

Ragavan, S., & Schoenborn, B. (1984) in *Neutrons in Biology* (Schoenborn, B. P., Ed.) Plenum Press, New York.

Richardson, J. (1981) *Adv. Protein Chem. 34*, 168–339.

Roder, H., Wagner, G., & Wüthrich, K. (1985) *Biochemistry 24*, 7396–7407.

Teeter, M., & Kossiakoff, A. (1984) in *Neutrons in Biology* (Schoenborn, B. P., Ed.) Plenum Press, New York.

Tüchsen, E., & Ottesen, M. (1979) *Carlsberg Res. Commun. 44*, 1–10.

Tüchsen, E., & Woodward, C. (1985a) *J. Mol. Biol. 185*, 405–419.

Tüchsen, E., & Woodward, C. (1985b) *J. Mol. Biol. 185*, 421–430.

Tüchsen, E., & Woodward, C. (1987a) *Biochemistry 26*, 8073–8078.

Tüchsen, E., & Woodward, C. (1987b) *J. Mol. Biol. 193*, 793–802.

Tüchsen, E., Hvidt, A., & Ottesen, M. (1980) *Biochemie 62*, 563–566.

Tüchsen, E., Hayes, J., Ramaprasad, S., Copie, V., & Woodward, C. (1987) *Biochemistry 26*, 5363–5172.

Woodward, C., & Hilton, B. (1980) *Biophys. J. 32*, 561–575.

Woodward, C., Simon, I., & Tüchsen, E. (1982) *Mol. Cell. Biochem. 48*, 135–160.

Wagner, G., & Wüthrich, K. (1979) J. Mol. Biol. 130, 31-37.
Wagner, G., & Wüthrich, K. (1982) J. Mol. Biol. 160, 343-361.
Walter, J., & Huber, R. (1983) J. Mol. Biol. 167, 911-917.
Wlodawer, A., & Sjolin, L. (1982) Proc. Natl. Acad. Sci. U.S.A. 79, 1418-1422.
Wlodawer, A., Walter, J., Huber, R., & Sjölin, L. (1984) J. Mol. Biol. 180, 301-329.
Wlodawer, A., Deisenhofer, J., & Huber, R. (1987a) J. Mol. Biol. 193, 145-156.
Wlodawer, A., Nachman, J., Gilliland, G., Gallagher, W., & Woodward, C. (1987b) J. Mol. Biol. 198, 469-480.

Apple Four in Human Blood Coagulation Factor XI Mediates Dimer Formation†

Joost C. M. Meijers,‡,§ Eileen R. Mulvihill,‖ Earl W. Davie,*,§ and Dominic W. Chung§
Department of Biochemistry, University of Washington, Seattle, Washington 98195, and Zymogenetics Inc., 4225 Roosevelt Way N.E., Seattle, Washington 98105

Received December 27, 1991; Revised Manuscript Received February 27, 1992

ABSTRACT: Human blood coagulation factor XI is a dimer composed of two identical subunits. Each subunit contains four apple domains as tandem repeats followed by a serine protease region. A disulfide bridge between Cys321 of each fourth apple domain links the subunits together. The role of Cys321 in the dimerization of factor XI was examined by mutagenesis followed by expression of its cDNA in baby hamster kidney cells. The recombinant proteins were then purified from the tissue culture medium and shown to have full biological activity. Normal recombinant factor XI was secreted as a dimer as determined by SDS-PAGE, while recombinant factor XI-Cys321Ser migrated as a monomer under these conditions. Gel filtration studies, however, revealed that each protein existed as a dimer under native conditions, indicating that the disulfide bond between Cys321 of each factor XI monomer was not necessary for dimer formation. The fourth apple domain (apple4) of factor XI was then introduced into tissue plasminogen activator (tPA) to investigate its role in the dimerization of other polypeptide chains. The fusion protein, containing apple4 (apple4-tPA), formed dimers as detected by SDS-PAGE and gel filtration. Furthermore, dimerization was specific to apple4, while apple3 had no effect on dimerization. These data further indicated that the apple4 domain of factor XI mediates dimerization of the two subunits and the interchain disulfide bond involving Cys321 was not essential for dimer formation.

Factor XI is a zymogen of a serine protease that participates in the intrinsic or contact phase of the blood coagulation cascade (Davie et al., 1991). Human factor XI is a glycoprotein that consists of two identical polypeptide chains held together by a single disulfide bond. Factor XI is activated by thrombin in the presence of a negatively charged surface (Naito & Fujikawa, 1991; Gailani & Broze, 1991), or by factor XIIa in the presence of high molecular weight kininogen and a polyanionic surface (Davie et al., 1979). Factor XIa is composed of two heavy and two light chains, which are held together by three disulfide bonds (McMullen et al., 1991). Each of the light chains contains the catalytic portion of the enzyme and is homologous to the pancreatic trypsin. Each of the heavy chains consists of 4 apple domains of 90 (or 91) amino acids (Fujikawa et al., 1986), and each apple domain has 3 characteristic disulfide bonds (McMullen et al., 1991). Several biological functions have been attributed to the apple domains. The first apple domains are involved in the binding of factor XI to high molecular weight kininogen (van der Graaf et al., 1983; Baglia et al., 1990), while the second apple domains are responsible for the calcium-dependent binding of factor XI to factor IX, its substrate (Sinha et al., 1985; Baglia et al., 1991). Each of the first and fourth apple domains contains an additional Cys residue. The two Cys residues at position 321 are linked together by a disulfide bond to form a homodimer.

In a previous study, the type III mutation of factor XI, in which Phe283 in the fourth apple domain was substituted by Leu (Asakai et al., 1989), was shown to be impaired in dimerization and secretion (Meijers et al., 1992). These results suggested that the fourth apple domains may be important in dimerization. In the present study, the role of Cys321 and the fourth apple domains in dimerization was examined.

Materials and Methods

Materials. Human factor XI and human plasma prekallikrein were purified according to previously published methods (Naito & Fujikawa, 1991; van der Graaf et al., 1982). The expression plasmids pZEM229R (Mulvihill et al., 1988) and ZpL7 (Johannessen et al., 1990) have been described. Prestained and [^{14}C]-labeled molecular weight markers were obtained from Bethesda Research Laboratories.

Construction of Factor XI Expression Vectors. The expression vector pZEM229R-XI was used for the expression of normal factor XI (Meijers et al., 1992). For mutagenesis of the cysteine residues, the human factor XI cDNA in M13mp18 was used (Meijers et al., 1992). Oligonucleotide primers PXI-M1 (AAGGACACCAGCTTTGAAGGA) and PXI-M2 (GCCCAAGCATCCAGCAACGAAGGG) were synthesized on an Applied Biosystems synthesizer and employed for mutagenesis of amino acid residues 11 and 321 from Cys to Ser. Mutagenesis was performed using T7-GEN (USB), by the method of Vandeyar et al. (1988). The mutations in the cDNA were confirmed by dideoxy sequencing, and the new constructs were then cloned into pZEM229R.

† This work was supported by Research Grant HL16919 from the National Institutes of Health.
* Address correspondence to this author.
‡ Present address: Department of Haematology, University Hospital Utrecht, P.O. Box 85500, 3508 GA Utrecht, The Netherlands.
§ University of Washington.
‖ Zymogenetics Inc.

0006-2960/92/0431-4680$03.00/0